Cryptic species and host specificity in the bryozoan-associated hydrozoan Zanclea divergens (Hydrozoa, Zancleidae).

Cryptic species and host specificity in the bryozoan-associated hydrozoan *Zanclea divergens* (Hydrozoa, Zancleidae)

Davide Maggioni[1,2,*], Andrea Schiavo[1,2], Andrew N. Ostrovsky[3,4], Davide Seveso[1,2], Paolo Galli[1,2], Roberto Arrigoni[5], Michael L. Berumen[6], Francesca Benzoni[6], Simone Montano[1,2]

[1] Department of Earth and Environmental Sciences (DISAT), University of Milano-Bicocca, 20126 Milano, Italy

[2] Marine Research and High Education (MaRHE) Center, University of Milano-Bicocca, 12030 Faafu Magoodhoo, Republic of the Maldives

[3] Department of Palaeontology, University of Vienna, 1090 Vienna, Austria

[4] Department of Invertebrate Zoology, Saint Petersburg State University, 199034 Saint Petersburg, Russia

[5] Department of Biology and Evolution of Marine Organisms (BEOM), Stazione Zoologica Anton Dohrn Napoli, 80121 Napoli, Italy

[6] Red Sea Research Center, Division of Biological and Environmental Science and Engineering, King Abdullah University of Science and Technology, 23955-6900 Thuwal, Saudi Arabia

* corresponding author: davide.maggioni@unimib.it

Abstract

Zanclea divergens is a tropical hydrozoan living in symbiotic association with bryozoans and currently reported from Papua New Guinea, Indonesia, and Maldives. Here, we used an integrative approach to assess the morpho-molecular diversity of the species across the Indo-Pacific. Phylogenetic and species delimitation analyses based on seven mitochondrial and nuclear loci revealed four well-supported molecular lineages corresponding to cryptic species, and representing a Pacific clade, an Indian clade, and two Red Sea clades. Since the general polyp morphology was almost identical in all samples, the nematocyst capsules were measured and analysed to search for possible fine-scale differences, and their statistical treatment revealed a significant difference in terms of length and width among the clades investigated. All *Zanclea divergens* specimens were specifically associated with cheilostome bryozoans belonging to the genus *Celleporaria*. The Pacific and Indian clades were associated with *Celleporaria* sp. and *C. vermiformis*, respectively, whereas both Red Sea lineages were associated with *C. pigmentaria*. Nevertheless, the sequencing of host bryozoans revealed that one of the Red Sea hydrozoan clades is associated with two morphologically undistinguishable, but genetically divergent, bryozoan species. Overall, our results show that *Z. divergens* is a species complex composed of morphologically cryptic lineages showing partially disjunct distributions and host specificity. The presence of two sympatric lineages living on the same host species reveal complex dynamics of diversification, and future research aimed at understanding their diversification process will likely improve our knowledge on the mechanisms of speciation among currently sympatric cryptic species.

Keywords

Species delimitation; Integrative taxonomy; Symbiosis; *Celleporaria*; Nematocysts

1. Introduction

Symbioses play a key role in the marine environment, and especially in coral reefs (Gates and Ainsworth, 2011), promoting the productivity (Muscatine and Porter, 1977), structural complexity (Bergsma, 2009; Bergsma and Martinez, 2011), and diversity of this ecosystem (Munday et al., 2004; Gittenberger and Gittenberger, 2011; Montano et al., 2015a). The symbionts can be associated to a single host, resulting in taxon-specific associations (*e.g.* Hoeksema et al., 2012; Montano et al., 2015b), but also generalism is a common phenomenon (*e.g.* Silverstein et al., 2012; Ivanenko et al., 2018). The diversity and phylogenetic patterns of some symbiotic taxa have been proposed to be the result of ecological speciation by host switch (Munday et al., 2004; Tsang et al., 2009, 2014; Maggioni et al., 2016), suggesting that the symbiotic lifestyle may boost symbiont speciation. In other cases, the genetic difference seems to be better explained by allopatric diversification, due to the presence of divergent closely related groups with same host but of differential distribution (Maggioni et al., 2017). Regardless of the mode of diversification, some of these symbiotic organisms show a morphological stasis despite high genetic diversification, and the presence of cryptic/sibling species has been largely documented (*e.g.* Gittenberger and Gittenberger, 2011; Harmelin et al. 2011, 2012; Van der Meij, 2015; Cáceres-Chamizo et al. 2017; Maggioni et al., 2017).

The hydrozoan family Zancleidae Russel, 1953 is a good candidate to explore the host- and geography-related diversification patterns in reef symbiotic organisms. Indeed, the genus *Zanclea* Gegenbaur, 1856 has a wide distribution, spanning from the tropics (Boero et al., 2000) to the poles (Peña Cantero et al., 2013), and polyps of most species live epibiotically on other organisms (Boero et al., 2000). Bryozoans are among the most common hosts for zancleids, and all representatives of the genera *Halocoryne* Hadzi, 1917 and *Zanclella* Boero and Hewitt, 1992 live in obligate association with them. Regarding *Zanclea*, 12 out of the 26 species with a described polyp stage live in obligate associations with bryozoans (Maggioni et al., 2018). The presence of cryptic species has been already reported in the genus *Zanclea*, in particular in coral-associated species (Montano et al., 2015a; Maggioni et al., 2017; Manca et al., 2019), and it has been hypothesised to be a common phenomenon rather than an exception in the group (Maggioni et al., 2018).

In the present work, we focused our attention on a poorly known *Zanclea* species: *Zanclea divergens* Boero, Bouillon and Gravili, 2000. This species was initially described from Laing Island, Papua New Guinea, in association with unidentified bryozoans (Boero et al., 2000). Later, it was reported from North Sulawesi, Indonesia, living on *Celleporaria sibogae* Winston and Heimberg, 1986 and another unidentified bryozoan (Puce et al., 2002), and from Maldives

associated with *Celleporaria vermiformis* (Waters, 1909) (Maggioni et al., 2020). Polyps and newly released medusae show typical *Zanclea* morphology, but the hydrorhiza is characterised by discrete clusters of nematocysts, interpreted by Boero et al. (2000) as a first tendency towards colony polymorphism. Similarly to other *Zanclea* symbioses (Montano et al., 2017; Osman and Haugsness, 1981), the interaction with the bryozoan seems to be mutualistic, as described by Puce et al. (2002), with both organisms benefiting from the association: bryozoans feed on the mucus released by hydroids and may obtain protection from their nematocysts, whereas hydroids are mechanically protected by the host.

In the present study, we used an integrative approach including multi-locus DNA taxonomy and phylogenetics, traditional morphology assessment, and statistical treatment of morphometric data to assess the morpho-molecular diversity of specimens of *Z. divergens* collected from four localities throughout the Indo-Pacific and associated with different host bryozoans that were also compared using molecular methods.

2. Material and methods

2.1 Sampling

Sampling was conducted between October 2014 and October 2019 in the Republic of Maldives, Saudi Arabian Red Sea, and Australian Great Barrier Reef (Fig. 1; Table S1). Fragments of bryozoans (*Celleporaria* spp.) bearing *Z. divergens* colonies were collected with hammer and chisel and thereafter placed in water bowls. Colonies were anesthetised with menthol crystals dissolved in seawater until hydrozoan polyps were fully extended. *Zanclea* hydranths were detached from the host bryozoans using syringe needles, precision forceps, and micropipettes, under a stereomicroscope. Afterwards, they were fixed in 99% ethanol and 10% formalin for molecular and morphological examinations, respectively. In a few cases, Maldivian specimens bearing medusa buds were kept in aquaria until medusae were released. Medusae were then fixed in 10% formalin for morphological analyses. Host bryozoans were also fixed in 99% ethanol for further analyses. Additionally, DNA of *Z. divergens* from Indonesia was obtained from the Muséum d'Histoire Naturelle of Geneva, Switzerland (specimen voucher: MHNG INVE:94102).

2.2. DNA extraction and sequencing, phylogenetic analyses

Total genomic DNA of ethanol-fixed hydrozoans and bryozoans was extracted following a protocol modified from Zietara et al. (2000). For hydrozoans, seven molecular markers were amplified, including three mitochondrial regions (16S rRNA, *COX1*, and *COX3*) and four

nuclear regions (18S rRNA, 28s rRNA, ITS, and *H3*), following the protocols described in Cunningham and Buss (1993), Folmer et al. (1994), Peña Cantero and Sentandreu (2016), Medlin et al. (1988), Maggioni et al. (2016), Fontana et al. (2012), and Colgan et al. (1998), respectively (Table 1). For bryozoans, a portion of the 16S rRNA was selected as molecular marker due to its suitability for both species level and higher taxonomic level analyses (Hao et al., 2005; Knight et al., 2010), and was amplified using the primers and protocol described in Palumbi et al. (1991). All PCR products were checked through electrophoretic runs in 1.5 % agarose gels, purified, and sequenced in forward and reverse directions using ABI 3730xl DNA Analyzer (Applied Biosystems). Geneious 6.1.6 was used to visually check and assemble the obtained sequences, and to translate protein-coding genes (*COX1*, *COX3*, and *H3*) to check for the presence of stop codons. The sequences obtained were deposited in GenBank (Table S1).

According to Maggioni et al. (2018), three outgroups were selected for the *Z. divergens* datasets, namely *Zanclea* sp. 2, *Asyncoryne ryniensis* Warren, 1908, and *Solanderia secunda* (Inaba, 1892). *Microporella ciliata* (Pallas, 1776) and *Celleporina souleae* Morris, 1979 (GenBank accession numbers: AF156286 and AF156279, respectively) were selected as outgroups for the bryozoan dataset (Hao et al., 2005). Sequences of each marker were aligned with MAFFT 7.110 (Katoh and Standley, 2013) using the *E-INS-i* option. The ITS dataset was further run through Gblocks (Castresana, 2000; Talavera and Castresana, 2007) using the default 'less stringent' settings to remove ambiguously aligned regions. General statistics of the obtained *Z. divergens* and *Celleporaria* spp. sequences and the variability of the employed molecular markers were calculated with DnaSP 6 (Rozas et al., 2017) (Table 1). All hydrozoan datasets were then concatenated using Mesquite 3.2 (Maddison and Maddison, 2006). Appropriate partition schemes and models were determined using jModelTest 2 (Darriba et al., 2012) for single-locus datasets (Table 1), and PartitionFinder 2 (Lanfear et al., 2012) for the multi-locus datasets, using the Akaike Information Criterion (AIC), the corrected AIC (AICc), and the Bayesian Information Criterion (BIC) (Table S2). Phylogenetic inference analyses were performed for all single- and multi-locus datasets using two optimality criteria: Bayesian inference (BI) and maximum likelihood (ML). BI analyses were performed using MrBayes 3.2.6 (Ronquist et al., 2012): four parallel Markov Chain Monte Carlo runs (MCMC) were run for 10^7 generations, trees were sampled every 1000^{th} generation, and burn-in was set to 25%. Maximum likelihood trees were built with RAxML 8.2.9 (Stamatakis, 2014) using 1000 bootstrap replicates. All alignments, model and partition detections, and phylogenetic tree reconstructions were run on the CIPRES server (Miller et al., 2010).

2.3. Species delimitation

To explore the presence of *Z. divergens* cryptic species, three families of species delimitation techniques were employed for each single locus dataset, namely the Automatic Barcoding Gap Discovery (ABGD), the Poisson Tree Processes (PTP), and the Generalised Mixed Yule Coalescence (GMYC). All analyses were run on reduced datasets, in which identical haplotypes and outgroups were removed, as indicated in Fontaneto et al. (2015). Phylogenetic trees were built using RAxML and MrBayes as previously described. Additionally, for GMYC analyses ultrametric trees were built using BEAST 1.8.2 (Drummond et al., 2012). A coalescent tree prior and the heterogeneity of the mutation rates across lineages were set under an uncorrelated lognormal relaxed clock. Three replicate analyses were run for 10^8 million generations with a sampling frequency of 10,000 and were combined using LogCombiner 1.8.2 (Drummond et al., 2012) with a burn-in set to 25%. The maximum clade credibility trees were computed using TreeAnnotator 1.8.2 (Drummond et al., 2012). The ABGD delimitations (Puillandre et al., 2012) were run on the website abgd web (http://www.abi.snv.jussieu.fr/public/abgd/abgdweb.html). Parameters were set as follows: Pmin = 0.001, Pmax = 0.1, Steps = 100, X = 1, Nb bins = 100, and all the three available models were tested (*p*-distance, Kimura 2-parameter, and Jukes Cantor). Single-threshold PTP and bPTP analyses (Zhang et al., 2013) were performed on the website bPTP web server (http://species.h-its.org/ptp), using both ML and BI phylogenetic trees, and running analyses for 400,000 MCMC generations, with thinning value = 100 and burn-in = 0.25. Multiple-threshold PTP (mPTP) analyses (Kapli et al., 2017) were run on the website mPTP Webserver (https://mptp.h-its.org). Single-threshold (Pons et al., 2006), multiple-threshold (Monaghan et al., 2009), and bGMYC (Reid and Carstens, 2012) analyses were run using ultrametric trees and were performed in R 3.1.3 (R Core Team, 2013) using the packages 'Splits' (Ezard et al., 2009), 'Ape' (Paradis et al., 2004), and 'bGMYC' (Reid and Carstens, 2012).

Genetic distances were calculated for each recovered clade/putative species using MEGA X (Kumar et al., 2018). Intra- and inter-clade % uncorrected *p*-distances were calculated with 1000 bootstrap replicates.

Additionally, each putative species was named following the method by Morard et al. (2016). This method is based on the definition of basetypes and the use of their hierarchical phylogenetic structure to define levels of divergence below that of morphospecies. A basetype is a specific DNA substitution pattern observed within a single marker gene, whereas a basegroup is a set of basetypes and constitute the lowest MOTU level. The genetic variability between the basegroup and the morphospecies is used to identify intermediate levels at

different degrees of divergence, and any of these levels could be theoretically considered a species hypothesis. Similarly to Maggioni et al. (2017) we defined basetypes using sequence patterns in the widely used hydrozoan barcode gene 16S rRNA.

2.4. Species tree

The species tree for *Z. divergens* was computed using *BEAST (Heled and Drummond, 2010) in BEAST 2.2.0 (Bouckaert et al., 2014) run on the CIPRES server (Miller et al., 2010). The specimens were assigned to different species according to the species delimitation analyses and the outgroups were removed. Mitochondrial loci were considered as a single partition, whereas nuclear loci were kept separate, and best-fit evolutionary models were assigned according to PartitionFinder 2 analyses. Yule process prior was used, together with a linear and constant-root population-size model. Each analysis ran for 10^8 generations, sampling every 10,000 generations, and 25% was set as burn-in. The species trees were visualised and edited in DensiTree 2.2.0 (Bouckaert and Heled, 2014) to qualitatively assess gene trees discordance.

2.5 Morphological and statistical analyses

Zanclea divergens specimens were firstly observed and photographed under Leica EZ4 D stereomicroscope to assess their general morphology, and subsequently analysed under Zeiss Axioskop 40 compound microscope to study the fine-scale morphology of polyps and medusae. The type and size of nematocysts were recorded and measured using ImageJ 1.52p software in order to compute further statistical analyses. Only specimens collected in the Maldives and Red Sea were included in the statistical analyses, since insufficient material was available for the sample from Australia. The three types of nematocysts found in *Z. divergens* polyps (stenoteles of two size classes and euryteles) were measured in their major and minor axes. Differences in the length and width of capsules among *Zanclea* specimens belonging to different genetic lineages were tested using one-way analysis of variance (ANOVA) when data were normally distributed, and non- parametric Kruskal-Wallis tests when data were not normally distributed. Parametric Tukey's HSD multiple comparison post hoc tests and non-parametric Mann–Whitney U-tests were performed to assess the significance of individual factors. All analyses were performed using SPSS 25. All data are presented as mean ± standard deviation.

In order to identify host-bryozoan species, tissues were removed from skeletons by immersion in a 10% sodium hypochlorite solution for 6-24 hours. Skeletons were then rinsed, air-dried, and sputter- coated with gold, to be observed under Zeiss Gemini SEM 500 scanning electron microscope.

3. Results

A total of 29 *Z. divergens* colonies associated with cheilostome bryozoans *C. vermiformis*, *C. pigmentaria* (Waters, 1909), and *Celleporaria* sp. were collected from the studied localities (13 from the Saudi Arabian Red Sea, 15 from Maldives, and one colony from Australia, Great Barrier Reef). All colonies were used for molecular analyses, whereas 18 colonies were selected for further morphological characterisation depending on their preservation (Table S1).

3.1. Phylogenetic and species delimitation analyses

Genomic DNA was successfully extracted from all samples and a total of 231 sequences were generated, including outgroups (Table S1). Mitochondrial loci showed the highest haplotype and nucleotide diversity, compared to the nuclear loci (Table 1), with the hydrozoan 16S rRNA being the most diverse DNA region among the analysed ones. jModelTest and PartitionFinder found slightly different best-fit evolutionary models according to the information criteria used (Table 1, Table S2), but the use of different models did not influence downstream analyses, resulting in highly similar phylogenetic trees. Similarly, the tree topologies of ML and BI analyses were highly consistent.

All *Z. divergens* samples formed a monophyletic clade, and apart from a few single-locus analyses, four lineages were recursively identified (Fig. 2, left side). According to the concatenated analyses, clade I is represented by the Indonesian and Australian samples and is sister to all other clades. Samples from the Red Sea (clades IIa and IIb) form two reciprocally monophyletic clades, sister to the Maldivian samples, which cluster in a single well-supported lineage (clade III). The described clades are found in all analyses except for single-locus 18S and 28S rRNA phylogenetic reconstructions, in which clades IIa and IIb cluster together and are not genetically differentiated. The bryozoan phylogenetic tree (Fig. 2, right side) resulted in four distinct *Celleporaria* clades showing high statistical supports, whereas a few internal nodes showed lower BI and ML support values. Maldivian samples (*C. vermiformis*) form a clade sister to all the other investigated samples. *Celleporaria pigmentaria* from the Red Sea is divided into two diverging lineages (*C. pigmentaria* 1 and *C. pigmentaria* 2), which differ from *Celleporaria* sp. from Australia. *Zanclea divergens* clade I is associated with the latter bryozoan species. Clades IIa and IIb are all associated with *C. pigmentaria* 2, except for one sample (FB325) associated with *C. pigmentaria* 1. Clade III from Maldives is always associated with *C. vermiformis*.

Zanclea divergens species delimitation results are summarised in Fig. 3. Apart from a few exceptions, the four lineages detected in the phylogenetic analyses were assigned to four different species hypotheses, with a general high level of agreement among the different methods. Mitochondrial regions and nuclear *H3* resolved better the species complex, whereas the 18S rRNA, 28S rRNA and ITS did not successfully distinguish clade IIa and IIb in most analyses. According to the molecular nomenclature system proposed by Morard et al. (2016), clade I was named *Z. divergens* I, clade IIa and IIb were named *Z. divergens* IIa and IIb, respectively, and clade III was named *Z. divergens* III.

Genetic distances between hydrozoan clades were generally high (Table 2), especially for mitochondrial markers, and further supported the assignment of each clade to different species hypotheses. Intra-clade distances were low and did not overlap with inter-clade distances (Table 2). Similarly, genetic distances between the bryozoan clades were high (9.2-20.4%), whereas intra-clade distances were extremely low, when calculable, supporting the fact that the four clades correspond to different species.

Finally, the *Z. divergens* species tree (Fig. 4) showed a topology in agreement with the tree resulting from the concatenated dataset (Fig. 2, left side), with no relevant discrepancies between gene trees, and with high support values.

3.2. Morphology of polyps and medusae

The general morphology of *Z. divergens* polyps was consistent with previous descriptions (Boero et al., 2000; Puce et al., 2002; Maggioni et al., 2020). All colonies were stolonal, monomorphic, and associated with cheilostome bryozoan species belonging to the genus *Celleporaria* (Fig. 5a-d). In all cases, the hydrorhiza extends below the bryozoan skeleton, projecting out in irregular clusters of nematocysts (Fig. 5e). Gastrozooids are cylindrical (Fig. 5f), reaching 3.5 mm in length, and coming out from holes in the calcified skeleton of the bryozoan, with the base and hydrorhiza partially overgrown by the host skeleton (Fig. 5g-h). When alive, polyps are transparent to whitish in colour, with white hypostomes (Fig. 5a-d). Oral tentacles are 4-6 in number, with large capitula (diameter: 82-40 µm), whereas 12-39 aboral tentacles with smaller capitula (diameter: 76-24 µm) are grouped in whorls of 4-5 along hydranth body and shorten proximally. Medusa buds were observed only for Maldivian specimens and develop in clusters directly from the hydrorhiza.

Maldivian newly released medusae (Fig. 5i) have a bell-shaped umbrella (diameter at release: 248-485 µm) with nematocysts on the surface and four radial exumbrellar nematocyst pouches. Pouches above the tentacular bulbs extend up to half of the exumbrella, whereas pouches on

the bulbs without tentacles are shorter. The manubrium is cylindrical, extending up to one third of the subumbrellar cavity, bearing nematocysts around the mouth. Two opposite tentacles (length at release: 530-1190 µm) are armed with 21-31 cnidophores, with 2-3 nematocysts each.

The polyp cnidome is composed of stenoteles of two size classes (Fig. 5j) (10-16 x 9-14 µm and 5-8 x 4-6 µm), distributed in tentacle capitula, and holotrichous macrobasic euryteles (Fig. 5k) (23-50 x 13-27 µm; shaft: 126-350 µm) around the hypostome and in hydrorhiza. The cnidome of the newly released medusa is composed of isorhizae (5-7 x 5-6 µm) on the exumbrella, bean-shaped holotrichous macrobasic euryteles (7-8 x 5-6 µm) in cnidophores, stenoteles of smaller size (5-8 x 4-6 µm) around the mouth, and stenoteles of larger size (12-16 x 11-13 µm) in the exumbrellar pouches. Morphological characteristics and nematocyst measurements for each *Z. divergens* clade are summarised in Tables 3, 4 and Tables S3, S4.

3.3. Statistical analyses of nematocysts measurements

A total of 53 polyps collected from 18 colonies belonging to *Z. divergens* IIa, IIb, and III were included in the statistical analyses and 1039 capsules were measured (391 large stenoteles, 386 small stenoteles, 262 euryteles) (Table S5). The statistical treatment of nematocyst measurements revealed differences between genetic lineages. Length and width of large stenoteles are significantly different among groups (Kruskal-Wallis $p<.0005$ for both). Mann-Whitney *U*-test revealed that length is higher in *Z. divergens* IIb than in the other two clades ($p<.0005$ for both comparisons), whereas all clades differ from each other in width ($p<.0005$ for all) (Fig. 6a). Small stenoteles showed differences in both length and width among lineages ($F_{2,382}=17.834$, $p<.0005$ and $F_{2,382}=19.382$, $p<.0005$, respectively). Tukey's HSD post hoc tests show that length and width are smaller in *Z. divergens* III than in *Z. divergens* IIa ($p<.0005$ and $p=.008$, respectively) and IIb (both $p<.0005$) (Fig. 6b). Length and width of euryteles differ among the three genetic lineages (Kruskal-Wallis $p<.0005$ for both). Specifically, *Z. divergens* IIb is larger than *Z. divergens* IIa and III in both length and width ($p<.0005$ for all) (Fig. 6c).

4. Discussion

Zanclea divergens is a species poorly represented in the special literature, with only four previous works focusing on its taxonomy or ecology (Boero et al., 2000; Puce et al., 2002; Di Camillo et al., 2008; Maggioni et al., 2020). Despite this lack of information, it has been reported as one of the most abundant hydrozoans in some localities (Di Camillo et al., 2008). Here, we widen the distributional range of this species, for the first time including the Red Sea

and the Great Barrier Reef, thus suggesting that its presence may be underestimated in other localities of the Indo-Pacific.

Phylogenetic analyses recursively revealed the presence of four well-supported hydrozoan lineages, and species delimitation analyses strongly supported their belonging to four different species. Therefore, *Z. divergens* is to be considered a species complex. The four clades show differences in their geographic distribution, although we admit that an addition of specimens from other localities may change the current scenario: *Z. divergens* I specimens inhabit the Pacific Ocean (Australia and Indonesia), *Z. divergens* IIa and IIb are found in the Red Sea, and *Z. divergens* III lives in the Indian Ocean (Maldives). Since the species was formerly described from Papua New Guinea (Boero et al., 2000), we may hypothesise that the holotype belongs to *Z. divergens* I, promoting the assignment of the name *Z. divergens* to the Pacific clade. However, the lack of molecular data from the type locality prevents further conclusions.

The four lineages here detected show nearly identical polyp morphology, consistent with the published descriptions of *Z. divergens*. Indeed, the general morphology of gastrozooids and newly released medusae (when observed), the presence of nematocyst clusters in the hydrorhiza, the position of medusa buds on the hydrorhiza, and the cnidome composition, fully agree with the original description (Boero et al., 2000) and subsequent re-descriptions (Puce et al., 2002; Maggioni et al., 2020) of *Z. divergens*. Additionally, as already reported for the Maldivian specimens (Maggioni et al., 2020), in all clades we found symbiont-related modifications of the host skeletons: the hydrorhiza extends for most of its length below the bryozoan skeleton, with polyps 'piercing' host colonies between zooids and being, in some cases, partially overgrown by a thin skeletal lamina.

In order to detect potential morphological differences among the four lineages, we compared the size of about 1000 nematocyst capsules (stenoteles of two size classes and euryteles). Similarly to other *Zanclea* species complexes (Manca et al., 2019), the statistical treatment of measurements revealed some fine-scale differences between the clades. *Zanclea divergens* I was not included in the analyses, due to the limited amount of available material, but all other lineages showed overall significant differences in nematocysts' length and width, even if differences in the individual factors were not consistent among cryptic species. The size of euryteles of *Z. divergens* I, despite not having been included in the statistical analyses, is larger than in the other two clades and is very similar to euryteles of *Z. divergens* described from Indonesia by Puce et al. (2002), indicating that the Pacific clade may have larger euryteles. Altogether, these morphological results support the importance of detailed cnidome analyses

in cnidarian taxonomy (e.g. González-Muñoz et al., 2017; Arrigoni et al., 2018; Manca et al., 2019).

Other than genetic and cnidome differences, the four *Z. divergens* lineages show different patterns of association with their hosts. According to our sampling and previous studies (Puce et al., 2002; Di Camillo et al., 2008), *Z. divergens* seems to be specifically associated with cheilostome bryozoans from the genus *Celleporaria*, namely *C. sibogae*, *C. pigmentaria*, *C. vermiformis*, and *Celleporaria* sp. The phylogenetic reconstruction and genetic distance analysis of host bryozoans showed the presence of four *Celleporaria* species, mostly corroborating the morphological identification. The 16S rRNA region allowed to clearly distinguish the morphospecies *C. pigmentaria*, *C. sibogae*, and *Celleporaria* sp., confirming its suitability for species-level analyses of bryozoan diversity, even if a few internal nodes showed low statistical support. Additionally, cryptic diversity was detected in *C. pigmentaria*, as this morphospecies was composed of two divergent and non-sister lineages showing high genetic distances, comparable to what observed for inter-specific comparisons in other bryozoan genera (e.g. Dick et al., 2003). Therefore, *C. pigmentaria* in the Red Sea represents a complex of at least two morphologically indistinguishable species.

Zanclea divergens I was found on the unidentified species *Celleporaria* sp. in Australia, genetically divergent from the other *Celleporaria* species. The Maldivian *Z. divergens* III was always found on *C. vermiformis*, and *Z. divergens* IIa and IIb were both associated with *C. pigmentaria*. Specifically, *Z. divergens* IIa was associated with only one of the *C. pigmentaria* lineages, whereas *Z. divergens* IIb was found on bryozoans belonging to both lineages. A hypothesis could be that the Red Sea *Z. divergens* was originally associated with a single species of *C. pigmentaria* and, at some point, two lineages (*Z. divergens* IIa and IIb) started to differentiate. When the diversification of the two *C. pigmentaria* lineages happened, *Z. divergens* IIb (but not *Z. divergens* IIa) was inherited by both bryozoan siblings. Alternatively, the association with both *C. pigmentaria* clades may be the result of a host range expansion of *Z. divergens* IIb occurred after the diversification of the two *C. pigmentaria* lineages, and this may have also favoured the divergence between the two Red Sea *Z. divergens* groups. However, the finding of only one colony of *C. pigmentaria* 1 limits further conclusions and future studies may elucidate the observed pattern. Host-specificity (both at the genus and species level) is a common phenomenon in zancleid species and some are obligate symbionts of their hosts (e.g. Piraino et al., 1992; Schuchert, 1996; Montano et al., 2015a, b). However, the association is generally not obligate for the host, and the same host can be associated with multiple *Zanclea* species, even if the co-occurrence of two species on the same host colony has

never been reported. For instance, the bryozoan *Rhynchozoon larreyi* (Audouin, 1826) hosts *Zanclea polymorpha* Schuchert, 1996 in New Zealand and *Zanclea retractilis* Boero, Bouillon & Gravili, 2000 in Papua New Guinea (Schuchert, 1996; Boero et al., 2000). A similar situation is observed for the bryozoan *C. pigmentaria*, which hosts *Zanclea* sp. 1 (*sensu* Maggioni et al., 2018) in the Maldives (Maggioni et al., 2020) and two *Z. divergens* lineages in the Red Sea.

According to our integrative approach, *Z. divergens* appears to be a complex of cryptic species, at least looking at the morphologically very similar polyp stages, with partially disjunct distribution and host-specificity. *Zanclea divergens* I and III are not only found in different localities, but also associated with different bryozoans. Their diversification may have occurred due to allopatric speciation, host shift, or a combination of both processes. Contrarily, *Z. divergens* IIa and IIb occupy the same host, have overlapping distributions, and likely exploit the same niches and resources. Sympatric cryptic species have been largely reported in literature (Knowlton, 1993) and in many cases they have been shown to be ecologically differentiated (Fišer et al., 2018), for instance in their host specificity (*e.g.* Maggioni et al., 2016) or reproductive timing (Villanueva, 2016). *Zanclea diverges* IIa and IIb may show reproductive isolation, even though they are not completely differentiated in slow-evolving nuclear loci (18S and 28S rRNA), and this may reflect a still ongoing (but limited) gene flow.

Overall, the four cryptic species showed a certain level of diversification in their cnidome, distributional ranges, and host specificity, but this variation was not always consistent in the four lineages. Together with the presence of *Zanclea* species described based on their adult medusa stage alone and the lack of genetic information for most *Zanclea* species, we preferred to cautiously avoid the formal naming of the species. However, the use of the nomenclatural system proposed by Morard et al. (2016) will allow the transfer of the acquired knowledge across disciplines, preventing the risk to create parallel taxonomical universes.

In conclusion, the results presented in this work widen the distributional range of the morphospecies *Z. divergens*, a symbiotic hydrozoan specifically associated with *Celleporaria* bryozoans in the Indo-Pacific and Red Sea. Integrative taxonomy analyses clearly revealed the presence of cryptic or possibly pseudo-cryptic species inhabiting partially different localities and hosts. The presence of two sympatric Red Sea lineages living on the same *Celleporaria* species reveal complex dynamics of diversification, and future research aimed at understanding their diversification process will likely provide useful information on the mechanisms of speciation between currently co-occurring cryptic species.

Acknowledgements

Authors are grateful to Peter Schuchert for sharing information and DNA of *Z. divergens* I, Tullia Isotta Terraneo (KAUST) and Malek Amr Gusti (KAUST) for logistic support during sampling in Saudi Arabia, and Timothy Ravasi (OIST) as co-organizer of the Farasan Banks Expedition in Saudi Arabia. We also thank Andrew Baird (ARC Centre of Excellence for Coral Reef Studies Grant # COE140100020 and DP180103199) for funding during sampling in the GBR. . This research was undertaken in accordance with the policies and procedures of KAUST. Permissions relevant to undertake the research have been obtained from the applicable governmental agencies. This project was partially supported by funding from PADI foundation (# 28634).

Declarations of interest: none

Appendix A. Supplementary material

Supplementary data associated with this article can be found, in the online version, at xxx.

References

Arrigoni, R., Maggioni, D., Montano, S., Hoeksema, B.W., Seveso, D., Shlesinger, T., Terraneo, T.I., Tietbohl, M.D., Berumen, M.L., 2018. An integrated morpho-molecular approach to delineate species boundaries of *Millepora* from the Red Sea. Coral Reefs, 37, 967–984. https://doi.org/10.1007/s00338-018-01739-8.

Bergsma, G.S., 2009. Tube-dwelling coral symbionts induce significant morphological change in *Montipora*. Symbiosis 49, 143–150. https://doi.org/10.1007/s13199-009-0047-5.

Bergsma, G.S., Martinez, C.M., 2011. Mutualist-induced morphological changes enhance growth and survival of corals. Mar. Biol. 158, 2267–2277. https://doi.org/10.1007/s00227-011-1731-6.

Boero, F., Bouillon, J., Gravili, C. 2000., A survey of *Zanclea*, *Halocoryne* and *Zanclella* (Cnidaria, Hydrozoa, Anthomedusae, Zancleidae) with description of new species. It. J. Zool. 67, 93–124. https://doi.org/10.1080/11250000009356301.

Bouckaert, R., Heled, J., 2014. DensiTree 2: Seeing Trees Through the Forest. bioRxiv. http://dx.doi.org/10.1101/012401.

Bouckaert, R., Heled, J., Kühnert, D., Vaughan, T., Wu, C.H., Xie, D., Suchard, M.A., Rambaut, A., Drummond, A.J., 2014. BEAST 2: a software platform for Bayesian evolutionary analysis. PLoS Comput. Biol. 10, e1003537. https://doi.org/10.1371/journal.pcbi.1003537.

Cáceres-Chamizo, J.P., Sanner, J.A., Tilbrook, K.J., Ostrovsky, A.N., 2017. Revision of the Recent species of *Exechonella* Canu & Bassler in Duvergier, 1924 and *Actisecos* Canu & Bassler, 1927 (Bryozoa, Cheilostomata): systematics, biogeography and evolutionary trends in skeletal morphology. Zootaxa, 4305, 1–79. http://dx.doi.org/10.11646/zootaxa.4305.1.1.

Castresana, J., 2000. Selection of conserved blocks from multiple alignments for their use in phylogenetic analysis. Mol. Biol. Evol. 17, 540–552. https://doi.org/10.1093/oxfordjournals.molbev.a026334.

Colgan, D., McLauchlan, A., Wilson, G., Livingston, S., Edgecombe, G., Macaranas, J., Gray, M., 1998. Histone H3 and U2 snRNA DNA sequences and arthropod molecular evolution. Aust. J. Zool. 46, 419–437. https://doi.org/10.1071/ZO98048.

Cunningham, C.W., Buss, L.W., 1993. Molecular evidence for multiple episodes of paedomorphosis in the family Hydractiniidae. Biochem. Syst. Ecol. 21, 57–69. https://doi.org/10.1016/0305-1978(93)90009-G.

Darriba, D., Taboada, G.L., Doallo, R., Posada, D., 2012. jModelTest 2: more models, new heuristics and parallel computing. Nat. Methods 9, 772. https://doi.org/10.1038/nmeth.2109.

Di Camillo, C.G., Bavestrello, G., Valisano, L., Puce, S., 2008. Spatial and temporal distribution in a tropical hydroid assemblage. J. Mar. Biol. Assoc. U.K. 8, 1589–1599. https://doi.org/10.1017/S0025315408002981.

Dick, M.H., Herrera-Cubilla, A., Jackson, J.B., 2003. Molecular phylogeny and phylogeography of free-living Bryozoa (Cupuladriidae) from both sides of the Isthmus of Panama. Mol. Phylogenet. Evol. 27, 355–371. https://doi.org/10.1016/S1055-7903(03)00025-3.

Drummond, A.J., Suchard, M.A., Xie, D., Rambaut, A., 2012. Bayesian phylogenetics with BEAUti and the BEAST 1.7. Mol. Biol. Evol. 29, 1969–1973. https://doi.org/10.1093/molbev/mss075.

Ezard, T., Fujisawa, T., Barraclough, T.G., 2009. SPLITS: Species Limits by threshold statistics. R Package Version 1.0-11. http://r-forge.r-project.org/projects/splits/

Fišer, C., Robinson, C. T., Malard, F., 2018. Cryptic species as a window into the paradigm shift of the species concept. Mol. Ecol. 27, 613–635. https://doi.org/10.1111/mec.14486.

Folmer, O., Black, M., Hoeh, W., Lutz, R., Vrijenhoek, R., 1994. DNA primers for amplification of mitochondrial cytochrome *c* oxidase subunit I from diverse metazoan invertebrates. Mol. Mar. Biol. Biotechnol. 3, 294–299.

Fontana, S., Keshavmurthy, S., Hsieh, H.J., Denis, V., Kuo, C-Y., Hsu, C-M., Chen, C.A., 2012. Molecular evidence shows low species diversity of coral-associated hydroids in *Acropora* corals. PloS One 7, e50130. https://doi.org/10.1371/journal.pone.0050130.

Fontaneto, D., Flot, J.F., Tang, C.Q., 2015. Guidelines for DNA taxonomy, with a focus on the meiofauna. Mar. Biodivers. 45, 433–451. https://doi.org/10.1007/s12526-015-0319-7.

Gates, R.D., Ainsworth, T.D., 2011. The nature and taxonomic composition of coral symbiomes as drivers of performance limits in scleractinian corals. J. Exp. Mar. Biol. Ecol. 408, 94–101. https://doi.org/10.1016/j.jembe.2011.07.029.

Gittenberger, A., Gittenberger, E., 2011. Cryptic, adaptive radiation of endoparasitic snails: sibling species of *Leptoconchus* (Gastropoda: Coralliophilidae) in corals. Org. Divers. Evol. 11, 21–41. https://doi.org/10.1007/s13127-011-0039-1

González-Muñoz, R., Garese, A., Tello-Musi, J.L., Acuña, F.H., 2017. Morphological variability of the "Caribbean hidden anemone" *Lebrunia coralligens* (Wilson, 1890). Zoomorphology, 136, 287–297. https://doi.org/10.1007/s00435-017-0352-0.

Hao, J., Li, C., Sun, X., Yang, Q., 2005. Phylogeny and divergence time estimation of cheilostome bryozoans based on mitochondrial 16S rRNA sequences. Chinese Sci. Bull. 50, 1205–1211. https://doi.org/10.1007/BF03183694.

Harmelin, J.G., Ostrovsky, A.N., Cáceres-Chamizo, J.P., Sanner, J., 2011. Bryodiversity in the tropics: taxonomy of *Microporella* species (Bryozoa Cheilostomata) with personate maternal zooids from Indian Ocean, Red Sea and southeast Mediterranean. Zootaxa, 2798, 1–30. http://dx.doi.org/10.11646/zootaxa.2798.1.1.

Harmelin, J.G., Vieira, L.M., Ostrovsky, A.N., Cáceres-Chamizo, J.P., Sanner, J.A., 2012. *Scorpiodinipora costulata* (Canu & Bassler, 1929) (Bryozoa, Cheilostomata), a taxonomic and biogeographic dilemma: complex of cryptic species or human-mediated cosmopolitan colonizer? Zoosystema, 34, 123–138. https://doi.org/10.5252/z2012n1a5.

Heled, J., Drummond, A.J., 2009. Bayesian inference of species trees from multilocus data. Mol. Biol. Evol. 27, 570–580. https://doi.org/10.1093/molbev/msp274.

Hoeksema, B.W., Van der Meij, S.E., Fransen, C.H., 2012. The mushroom coral as a habitat. J. Mar. Biol. Assoc. U.K. 92, 647–663. https://doi.org/10.1017/S0025315411001445.

Ivanenko, V.N., Hoeksema, B.W., Mudrova, S.V., Nikitin, M.A., Martínez,A., Rimskaya-Korsakova, N.N., Berumen, M.L., Fontaneto, D., 2018. Lack of host specificity of copepod crustaceans associated with mushroom corals in the Red Sea. Mol. Phylogenet. Evol. 127, 770–780. https://doi.org/10.1016/j.ympev.2018.06.024.

Kapli, P., Lutteropp, S., Zhang, J., Kobert, K., Pavlidis, P., Stamatakis, A., Flouri, T., 2017. Multi-rate Poisson tree processes for single-locus species delimitation under maximum likelihood and Markov chain Monte Carlo. Bioinformatics 33, 1630–1638. https://doi.org/10.1093/bioinformatics/btx025.

Katoh, K., Standley, D.M., 2013. MAFFT multiple sequence alignment software version 7: improvements in performance and usability. Mol. Biol. Evol. 30, 772–780. https://doi.org/10.1093/molbev/mst010.

Knight, S., Gordon, D.P., Lavery, S.D., 2011. A multi-locus analysis of phylogenetic relationships within cheilostome bryozoans supports multiple origins of ascophoran frontal shields. Mol. Phylogenet. Evol. 61, 351–362. https://doi.org/10.1016/j.ympev.2011.07.005.

Knowlton, N., 1993. Sibling species in the sea. Annu. Rev. Ecol. Evol. Syst. 24, 189–216. https://doi.org/10.1146/annurev.es.24.110193.001201.

Kumar, S., Stecher, G., Li, M., Knyaz, C., Tamura, K., 2018. MEGA X: molecular evolutionary genetics analysis across computing platforms. Mol. Biol. Evol. 35, 1547–1549. https://doi.org/10.1093/molbev/msy096.

Lanfear, R., Calcott, B., Ho, S.Y., Guindon, S., 2012. PartitionFinder: combined selection of partitioning schemes and substitution models for phylogenetic analyses. Mol. Biol. Evol. 29, 1695–1701. https://doi.org/10.1093/molbev/mss020.

Maddison, W.P., Maddison, D.R., 2006. Mesquite: a modular system for evolutionary analysis. http://www.mesquiteproject.org

Maggioni, D., Montano, S., Seveso, D., Galli, P., 2016. Molecular evidence for cryptic species in *Pteroclava krempfi* (Hydrozoa, Cladocorynidae) living in association with alcyonaceans. Syst. Biodivers. 14, 484–493. https://doi.org/10.1080/14772000.2016.1170735.

Maggioni, D., Montano, S., Arrigoni, R., Galli, P., Puce, S., Pica, D., Berumen, M.L., 2017. Genetic diversity of the *Acropora*-associated hydrozoans: new insight from the Red Sea. Mar. Biodivers. 47, 1045–1055. https://doi.org/10.1007/s12526-017-0632-4.

Maggioni, D., Arrigoni, R., Galli, P., Berumen, M.L., Seveso, D., Montano, S., 2018. Polyphyly of the genus *Zanclea* and family Zancleidae (Hydrozoa, Capitata) revealed by the integrative analysis of two bryozoan-associated species. Contr. Zool. 87, 87–104. https://doi.org/10.1163/18759866-08702003.

Maggioni, D., Saponari, L., Seveso, D., Galli, P., Schiavo, A., Ostrovsky A.N., Montano, S., 2020. Green fluorescence patterns in closely related symbiotic species of *Zanclea* (Hydrozoa, Capitata). Diversity 12, 78. https://doi.org/10.3390/d12020078.

Manca, F., Puce, S., Caragnano, A., Maggioni, D., Pica, D., Seveso, D., Galli, P., Montano, S., 2019. Symbiont footprints highlight the diversity of scleractinian- associated *Zanclea* hydrozoans (Cnidaria, Hydrozoa). Zool. Scr. 48, 399–410. https://doi.org/10.1111/zsc.12345.

Medlin, L., Elwood, H.J., Stickel, S., Sogin, M.L., 1988. The characterization of enzymatically amplified eukaryotic 16S-like rRNA-coding regions. Gene 71, 491–499. https://doi.org/10.1016/0378-1119(88)90066-2.

Miller, M.A., Pfeiffer, W., Schwartz, T., 2010. Creating the CIPRES Science Gateway for inference of large phylogenetic trees. Proceedings of the Gateway Computing Environments Workshop. https://doi.org/10.1109/GCE.2010.5676129.

Monaghan, M.T., Wild, R., Elliot, M., Fujisawa, T., Balke, M., Inward, D.J., Vogler, A.P., 2009. Accelerated species inventory on Madagascar using coalescent-based models of species delineation. Syst. Biol. 58, 298–311. https://doi.org/10.1093/sysbio/syp027.

Montano, S., Maggioni, D., Arrigoni, R., Seveso, D., Puce, S., Galli, P., 2015a. The hidden diversity of *Zanclea* associated with scleractinians revealed by molecular data. PLoS One 10, e0133084. https://doi.org/10.1371/journal.pone.0133084.

Montano, S., Arrigoni, R., Pica, D., Maggioni, D., Puce, S., 2015b. New insights into the symbiosis between *Zanclea* (Cnidaria, Hydrozoa) and scleractinians. Zool. Scr. 44, 92–105. https://doi.org/10.1111/zsc.12081.

Montano, S., Fattorini, S., Parravicini, V., Berumen, M.L., Galli, P., Maggioni, Arrigoni, R., D., Seveso, D., Strona, G., 2017. Corals hosting symbiotic hydrozoans are less susceptible to predation and disease. Proc. R. Soc. B. 284, 20172405. https://doi.org/10.1098/rspb.2017.2405.

Morard, R., Escarguel, G., Weiner, A.K., Andre, A., Douady, C.J., Wade, C.M., de Garidel-Thoron, T., 2016. Nomenclature for the nameless: a proposal for an integrative molecular taxonomy of cryptic diversity exemplified by planktonic foraminifera. Syst. Biol. 65, 925–940. https://doi.org/10.1093/sysbio/syw031.

Munday, P.L., van Herwerden, L., Dudgeon, C.L., 2004. Evidence for sympatric speciation by host shift in the sea. Curr. Biol. 14, 1498–1504. https://doi.org/10.1016/j.cub.2004.08.029.

Muscatine, L., Porter, J.W., 1977. Reef corals: mutualistic symbioses adapted to nutrient-poor environments. Bioscience 27, 454–460. https://doi.org/10.2307/1297526.

Osman, R.W., Haugsness, J.A., 1981. Mutualism among sessile invertebrates: a mediator of competition and predation. Science 211, 846–848. https://doi.org/10.1126/science.211.4484.846.

Palumbi, S., 1991. Simple fool's guide to PCR. University of Hawaii.

Paradis, E., Claude, J., Strimmer, K., 2004. APE: analyses of phylogenetics and evolution in R language. Bioinformatics 20, 289–290. https://doi.org/10.1093/bioinformatics/btg412.

Peña-Cantero, Á.L., Boero, F., Piraino, S., 2013. Shallow-water benthic hydroids from Tethys Bay (Terra Nova Bay, Ross Sea, Antarctica). Polar Biol. 36, 731–753. https://doi.org/10.1007/s00300-013-1299-3.

Peña-Cantero, Á.L., Sentandreu, V., 2017. Phylogenetic relationships of endemic Antarctic species of *Staurotheca* Allman, 1888 (Cnidaria, Hydrozoa). Polar Biol. 40, 301–312. https://doi.org/10.1007/s00300-016-1954-6.

Piraino, S., Bouillon, J., Boero, F., 1992. *Halocoryne epizoica* (Cnidaria, Hydrozoa), a hydroid that" bites". Sci. Mar. 56, 141–147.

Pons, J., Barraclough, T.G., Gomez-Zurita, J., Cardoso, A., Duran, D.P., Hazell, V., Vogler, A.P., 2006. Sequence based species delimitation for the DNA taxonomy of undescribed insects. Syst. Biol. 55, 595–609. https://doi.org/10.1080/10635150600852011.

Puce, S., Cerrano, C., Boyer, M., Ferretti, C., Bavestrello, G., 2002. *Zanclea* (Cnidaria: Hydrozoa) species from Bunaken Marine Park (Sulawesi Sea, Indonesia). J. Mar. Biol. Assoc. U.K. 82, 943–954. https://doi.org/10.1017/S0025315402006434.

Puillandre, N., Lambert, A., Brouillet, S., Achaz, G., 2012. ABGD, Automatic Barcode Gap Discovery for primary species delimitation. Mol. Ecol. 21, 1864–1877. https://doi.org/10.1111/j.1365-294X.2011.05239.x.

R Core Team, 2013. R: A language and environment for statistical computing. R Foundation for Statistical Computing, Vienna, Austria <http://www.R-project.org/.

Reid, N.M., Carstens, B.C., 2012. Phylogenetic estimation error can decrease the accuracy of species delimitation: a Bayesian implementation of the general mixed Yule-coalescent model. BMC Evol. Biol. 12, 196. https://doi.org/10.1186/1471-2148-12-196.

Ronquist, F., Teslenko, M., van der Mark, P., Ayres, D.L., Darling, A., Höhna, S., Huelsenbeck, J.P., 2012. MrBayes 3.2: efficient Bayesian phylogenetic inference and model choice across a large model space. Syst. Biol. 61, 539–542. https://doi.org/10.1093/sysbio/sys029.

Rozas, J., Ferrer-Mata, A., Sánchez-DelBarrio, J.C., Guirao-Rico, S., Librado, P., Ramos-Onsins, S.E., Sánchez-Gracia, A., 2017. DnaSP 6: DNA sequence polymorphism analysis of large datasets. Mol. Biol. Evol. 34, 3299–3302. https://doi.org/10.1093/molbev/msx248.

Schuchert, P., 1996. The Marine Fauna of New Zealand: Athecate Hydroids and Their Medusae (Cnidaria (Vol. 106). New Zealand Oceanographic Institute.

Silverstein, R.N., Correa, A.M., Baker, A.C., 2012. Specificity is rarely absolute in coral–algal symbiosis: implications for coral response to climate change. Proc. R. Soc. B. 279, 2609–2618. https://doi.org/10.1098/rspb.2012.0055.

Stamatakis, A., 2014. RAxML version 8: a tool for phylogenetic analysis and post-analysis of large phylogenies. Bioinformatics 30, 1312–1313. https://doi.org/10.1093/bioinformatics/btu033.

Talavera, G., Castresana, J., 2007. Improvement of phylogenies after removing divergent and ambiguously aligned blocks from protein sequence alignments. Syst. Biol. 56, 564–577. https://doi.org/10.1080/10635150701472164.

Tsang, L.M., Chan, B.K.K., Shih, F.L., Chu, K.H., Chen, A.C., 2009. Host- associated speciation in the coral barnacle *Wanella milleporae* (Cirripedia: Pyrgomatidae) inhabiting the *Millepora* coral. Mol. Ecol. 18, 1463–1475. https://doi.org/10.1016/j.ympev.2014.03.002.

Tsang, L.M., Chu, K.H., Nozawa, Y., Chan, B.K.K., 2014. Morphological and host specificity evolution in coral symbiont barnacles (Balanomorpha: Pyrgomatidae) inferred from a multi-locus phylogeny. Mol. Phylogenet. Evol. 77, 11–22. https://doi.org/10.1016/j.ympev.2014.03.002.

Van Der Meij, S.E., 2015. Host relations and DNA reveal a cryptic gall crab species (Crustacea: Decapoda: Cryptochiridae) associated with mushroom corals (Scleractinia: Fungiidae). Contr. Zool. 84, 39–57. https://doi.org/10.1163/18759866-08401004.

Villanueva, R.D., 2016. Cryptic speciation in the stony octocoral *Heliopora coerulea*: temporal reproductive isolation between two growth forms. Mar. Biodivers. 46, 503–507. https://doi.org/10.1007/s12526-015-0376-y.

Zhang, J., Kapli, P., Pavlidis, P., Stamatakis, A., 2013. A general species delimitation method with applications to phylogenetic placements. Bioinformatics 29, 2869–2876. https://doi.org/10.1093/bioinformatics/btt499.

Zietara, M.S., Arndt, A., Geets, A., Hellemans, B., Volckaert, F. A., 2000. The nuclear rDNA region of *Gyrodactylus arcuatus* and *G. branchicus* (Monogenea: Gyrodactylidae). J.

Parasitol. 86, 1368–1373. https://doi.org/10.1645/0022-3395(2000)086[1368:TNRROG]2.0.CO;2.

Tables

Table 1. Primers, statistics, and evolutionary models used for each locus included in the analyses. Ns: number of sequences; S: number of sites; Sv: number of variable sites; M: number of mutations; H: number of unique haplotypes; Hd: haplotype diversity; Nd: nucleotide diversity. Hd and Nd are shown as mean ± standard deviation.

								Substitution models		
Region	Primers	Ns	S	Sv (M)	H	Hd	Nd	AIC	AICc	BIC
16S rRNA	SHB-SHA	30	561	91 (107)	22	0.973 ± 0.018	0.044 ± 0.004	GTR+I+G	GTR+I+G	GTR+G
COX1	LCO1490-HCO2198	20	653	143 (167)	15	0.963 ± 0.028	0.085 ± 0.008	GTR+I+G	GTR+I+G	GTR+I+G
COX3	CO3F-CO3R	20	564	94 (110)	12	0.937 ± 0.033	0.089 ± 0.008	GTR+I+G	GTR+I+G	HKY+G
18S rRNA	18SA-18SB	30	1670	17 (17)	5	0.628 ± 0.062	0.001 ± 0.000	GTR+I	GTR+I	HKY+I
28S rRNA	28SHF-R2077	30	1616	30 (30)	4	0.648 ± 0.062	0.005 ± 0.001	GTR+I	GTR+I	K80+I
ITS	HITSF-HITSR	30	520	38 (44)	6	0.722 ± 0.068	0.019 ± 0.003	HKY+I+G	HKY+I+G	K80+G
H3	H3F-H3R	29	352	26 (26)	6	0.695 ± 0.076	0.023 ± 0.003	HKY+I	HKY+I	K80+I
16S rRNA (bryozoa)	16AR-16BR	29	438	107 (124)	5	0.658 ± 0.066	0.110 ± 0.006	GTR+G	GTR+G	GTR+G

Table 2. Genetic distances (% uncorrected *p*-distances) between and within *Z. divergens* and *Celleporaria* species for each locus. Standard deviations are reported in parentheses.

16S rRNA					**28S rRNA**				
I	0.6 (0.3)				I	n.c.			
IIa	9.3 (1.3)	0.3 (0.1)			IIa	1.2 (0.3)	0.0 (0.0)		
IIb	9.0 (1.2)	5.6 (0.9)	0.3 (0.2)		IIb	1.3 (0.3)	0.0 (0.0)	0.0 (0.0)	
III	9.1 (1.2)	5.0 (0.9)	6.9 (1.0)	1.0 (0.2)	III	1.6 (0.3)	0.8 (0.2)	0.8 (0.2)	0.0 (0.0)
COX1					**ITS**				
I	n.c.				I	0.0 (0.0)			
IIa	14.1 (1.3)	1.2 (0.3)			IIa	6.2 (1.0)	0.1 (0.1)		
IIb	13.6 (1.4)	9.3 (1.0)	0.4 (0.2)		IIb	6.3 (1.0)	1.9 (0.5)	0.4 (0.2)	
III	14.6 (1.3)	13.3 (1.2)	10.5 (1.1)	2.3 (0.3)	III	5.6 (1.0)	2.9 (0.7)	3.5 (0.7)	0.0 (0.0)
COX3					***H3***				
I	n.c.				I	n.c.			
IIa	14.1 (1.4)	1.5 (0.4)			IIa	6.0 (1.4)	0.3 (0.2)		
IIb	14.2 (1.5)	9.7 (1.1)	0.4 (0.2)		IIb	5.3 (1.3)	2.9 (0.8)	0.2 (0.2)	
III	15.6 (1.4)	12.4 (1.3)	13.1 (1.4)	2.1 (0.4)	III	6.4 (1.4)	2.8 (0.9)	3.4 (0.9)	0.0 (0.0)
18S rRNA					**16S rRNA (*Celleporaria*)**				
I	0.4 (0.2)				*Celleporaria* sp.	n.c.			
IIa	0.7 (0.2)	0.1 (0.1)			*C. pigmentaria* 1	11.5 (1.5)	n.c.		
IIb	0.6 (0.2)	0.1 (0.1)	0.0 (0.0)		*C. pigmentaria* 2	9.2 (1.4)	9.4 (1.5)	0.1 (0.1)	
III	0.7 (0.2)	0.2 (0.1)	0.2 (0.1)	0.0 (0.0)	*C. vermiformis*	19.2 (1.9)	19.6 (1.9)	20.4 (1.9)	0.0 (0.0)

Table 3. Statistics of the measurements of large and small stenotele for the four *Z. divergens* lineages.

	Large stenotele length			**Large stenotele width**			**Small Stenotele length**			**Small stenotele width**		
Clade	**n**	**range**	**mean ± SD**	**n**	**range**	**mean ± SD**	**n**	**range**	**mean ± SD**	**n**	**range**	**mean ± SD**
I	8	14.6-16.1	15.3 ± 0.5	8	13.7-14.6	13.3 ± 0.9	7	5.9-7.3	5.3 ± 0.3	7	5.0-5.7	6.6 ± 0.6
IIa	44	11.4-14.4	13.0 ± 0.8	44	9.6-11.9	10.8 ± 0.6	46	5.9-8.0	6.8 ± 0.5	46	4.2-5.6	5.0 ± 0.3
IIb	123	13.2-16.4	14.8 ± 0.7	123	10.8-13.6	12.2 ± 0.6	127	5.8-7.8	6.8 ± 0.4	127	4.1-6.0	5.0 ± 0.3
III	228	9.6-15.4	13.3 ± 1.0	228	8.7-13.1	11.3 ± 0.7	221	5.4-7.9	6.6 ± 0.4	221	4.0-5-5	4.8 ± 0.3

Table 4. Statistics of the measurements of euryteles for the four *Z. divergens* lineages.

Clade	Eurytele length			Eurytele width			Eurytele shaft		
	n	range	mean ± SD	n	range	mean ± SD	n	range	mean ± SD
I	12	42.6-50.8	46.3 ± 3.0	12	22.5-27.4	24.8 ± 1.6	1	350	/
IIa	27	25.6-32.1	28.8 ± 2.0	27	13.7-18.4	15.3 ± 1.1	3	125.9-131.2	128.2 ± 2.8
IIb	84	23.0-33.9	30.5 ± 1.8	84	13.7-19.6	17.4 ± 1.1	3	152.1-164.8	159.0 ± 6.5
III	160	24.8-32.7	28.9 ± 1.6	160	12.6-17.6	14.9 ± 1.0	3	130.6-136.7	132.9 ± 3.3

Figure legends

Figure 1. Map of the sampling localities and currently known distribution of *Zanclea divergens*. The red label indicates the type locality of the species (not sampled). Yellow labels indicate area where samples were collected.

Figure 2. Phylogenetic trees of *Zanclea divergens* (left side) and host bryozoans (right side). The *Z. divergens* tree results from the seven-loci concatenated dataset and different clades are highlighted with different colours, whereas the *Celleporaria* tree results from the analysis of the *16S rRNA* region. Numbers at nodes represent Bayesian posterior probabilities and ML bootstrap values, respectively. Grids at nodes of the hydrozoan tree refer to single-locus analyses for both BI analysis (upper squares) and ML analysis (lower squares), and colours represent different statistical support, as shown in the legend. Each sample is represented by an alphanumeric code with information on the sampling locality, as shown in the legend. Dotted lines between the two trees indicate host-symbiont relationships.

Figure 3. Summary of the species delimitation analyses for each locus. Green colour indicates that the molecular clade was successfully delimited as a putative species, yellow colour indicates that the molecular clade was further subdivided in two or more lineages, red colour indicates that the molecular clade clustered with other lineages.

Figure 4. Species tree of the *Z. divergens* species complex. The cloudogram illustrates the posterior distribution of 10,000 trees inferred with *BEAST based on seven loci. High colour

density is indicative of areas in the tree with high topology agreement. The consensus tree is in white and numbers at nodes represent Bayesian posterior probabilities.

Figure 5. *Zanclea divergens* morphological characters. a) *Z. divergens* I on *Celleporaria* sp. from Australia. b, c) *Z. divergens* IIa and IIb, respectively, on *C. pigmentaria* 2 from Saudi Arabia. d) *Z. divergens* III on *C. vermiformis.* e) Hydrorhiza of *Z. divergens* III projecting out from the colony of *C. vermiformis* (arrowheads). f) Single *Z. divergens* III polyp detached from the host. g, h) Bryozoan skeletal modifications due to the presence of *Z. divergens* I (in *C. vermiformis*) and III (in *Celleporaria* sp.), respectively (arrowhead: skeletal lamina surrounding the hydrorhiza). i) Newly released medusa of *Z. divergens* III. j) Stenoteles of two size classes (black arrowhead: small stenotele; white arrowhead: large stenotele) and k) euryteles in the polyps of *Z. divergens* III. Scale bars: a, d) 1mm; b, c) 0.5 mm; e, f, h, i) 0.1 mm; g) 20 µm; j, k) 10 µm.

Figure 6. Box plots of a) large stenoteles, b) small stenoteles, and c) euryteles lengths and widths for *Z. divergens* IIa, IIb, and III. Boxes show the first and third quartiles, whiskers show range values, and horizontal lines indicate median values. Asterisks indicate statistically significant differences among the lineages.

Supplementary material

Table S1. Information on the specimens included in the analyses.

Table S2. Evolutionary models and partitions used for the concatenated dataset following the Akaike Information Criterion (AIC), corrected Akaike Information Criterion (cAIC), and Bayesian Information Criterion (BIC).

Table S3. Summary of *Z. divergens* measurements for each lineage.

Table S4. Measurements of nematocysts of the newly released medusa of *Z. divergens* III.

Table S5. Measurements of large and small stenoteles and euryteles of *Z. divergens* IIa, IIb, and III.

Figure 1

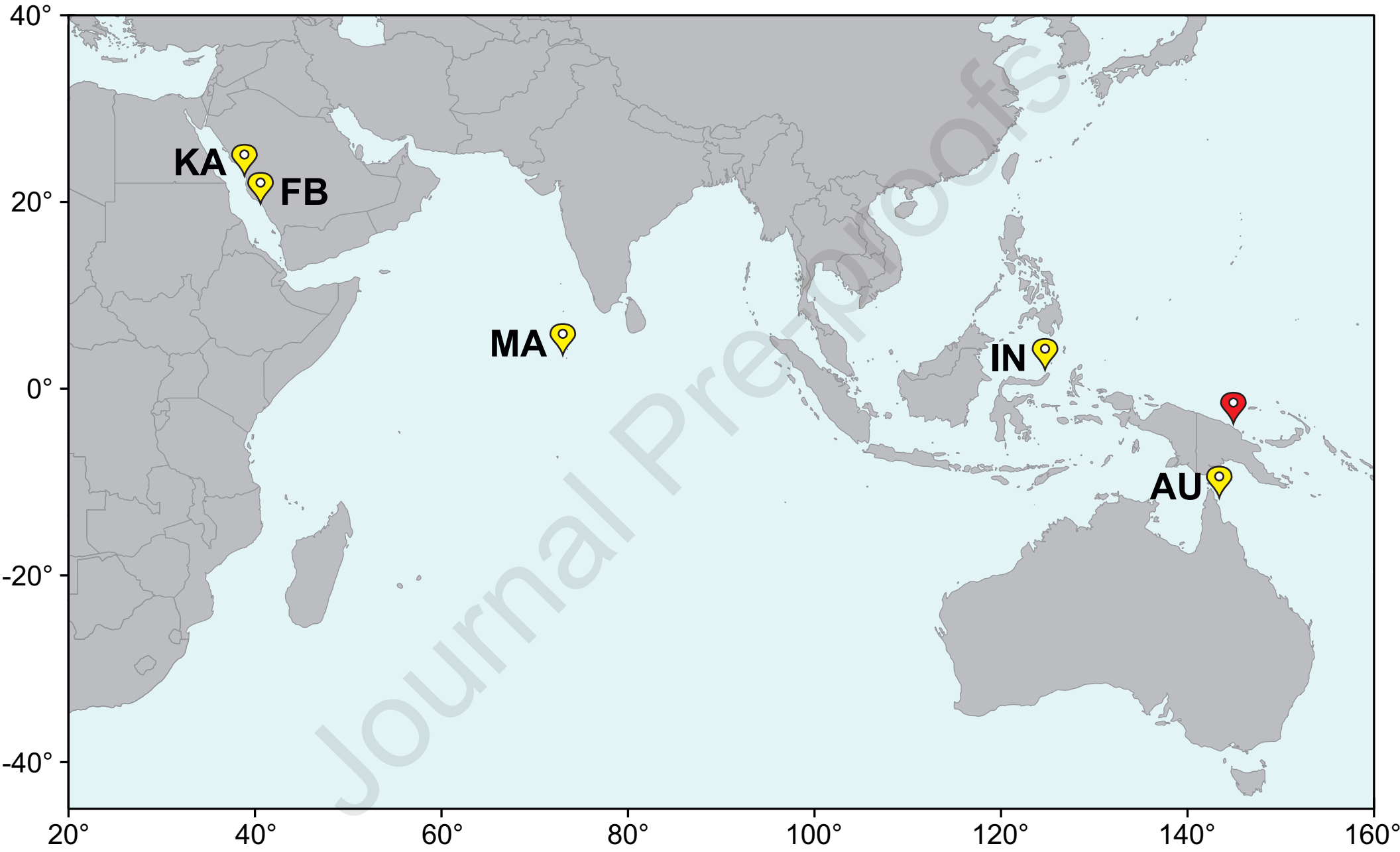

Figure 2

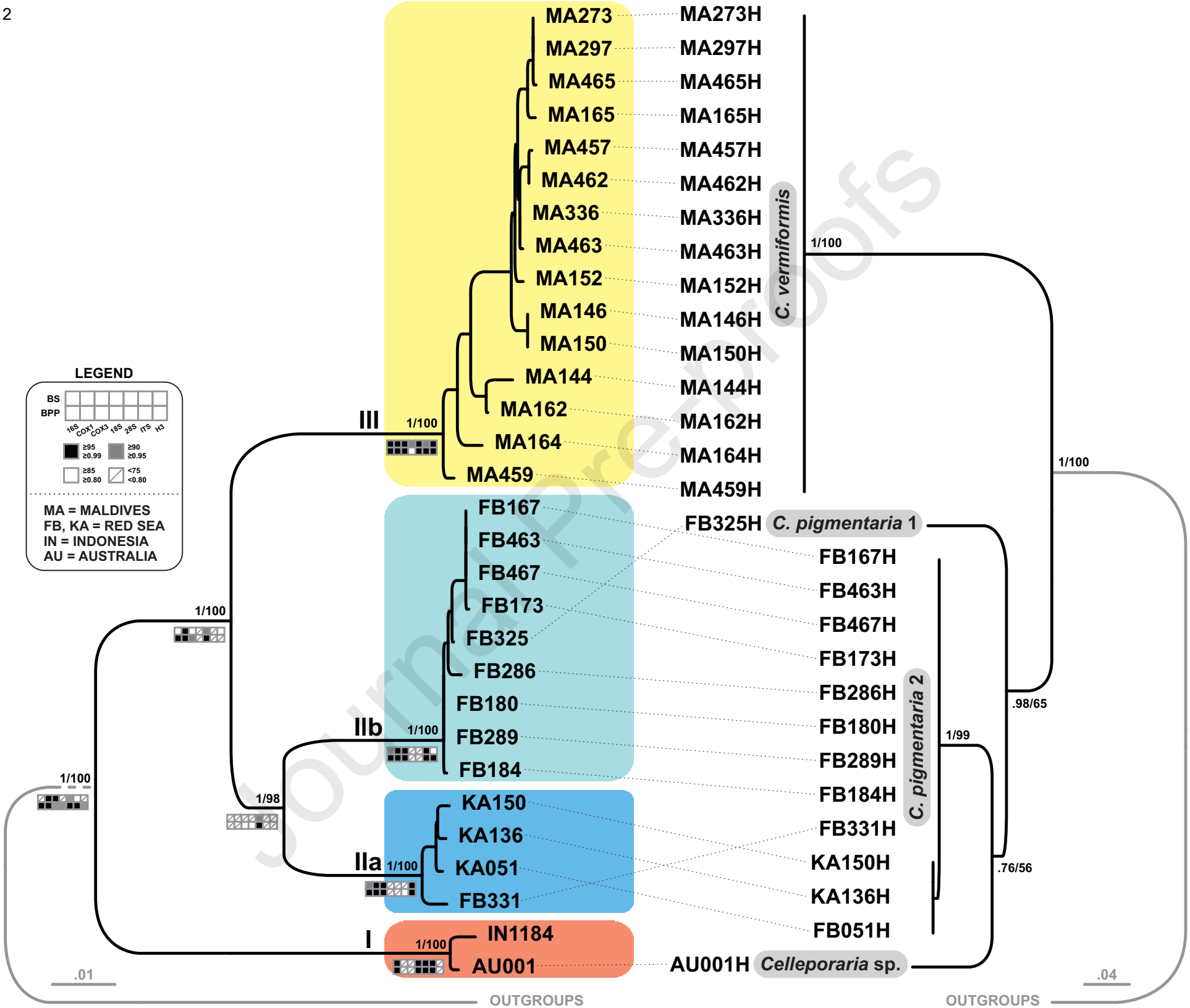

Figure 3

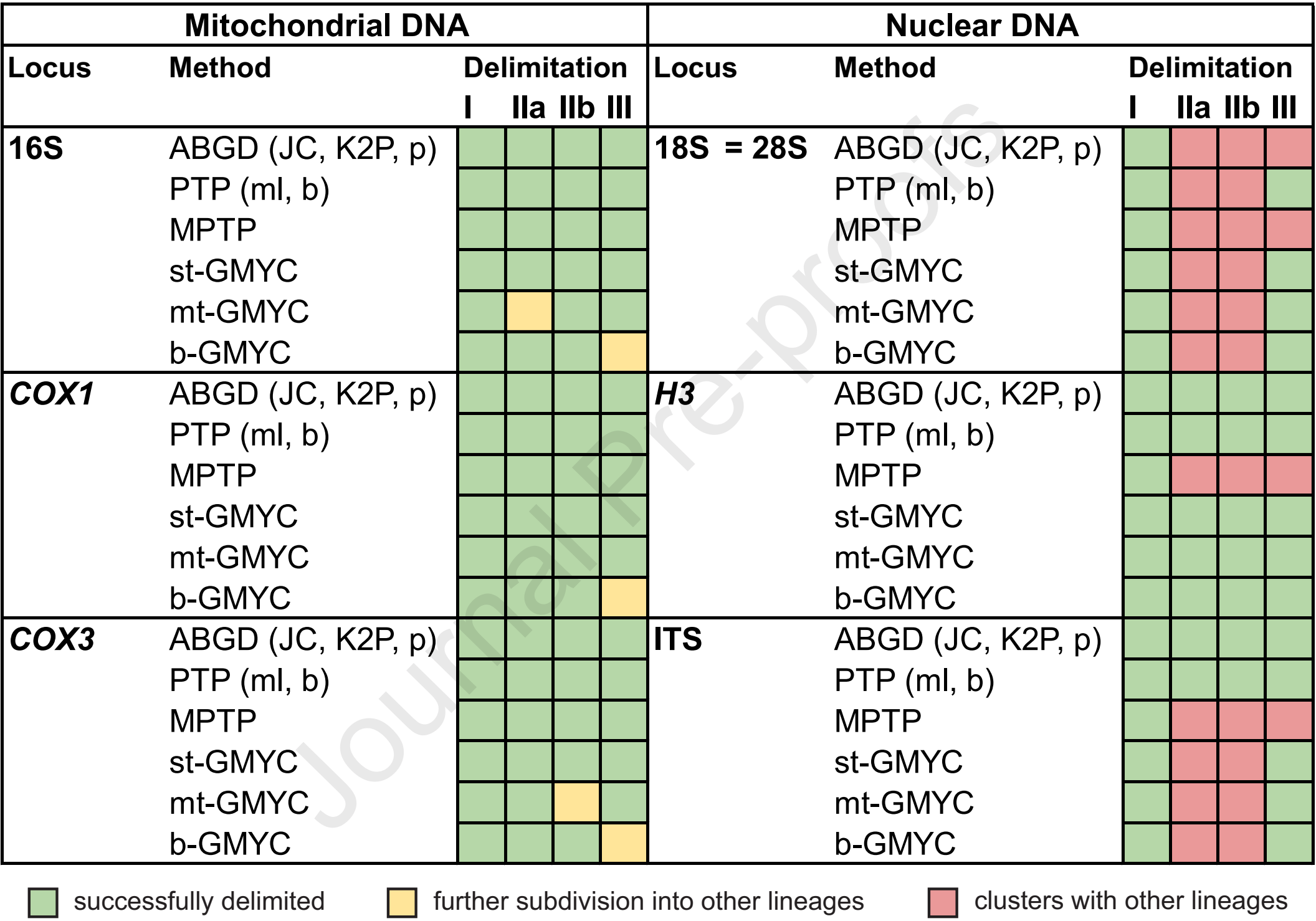

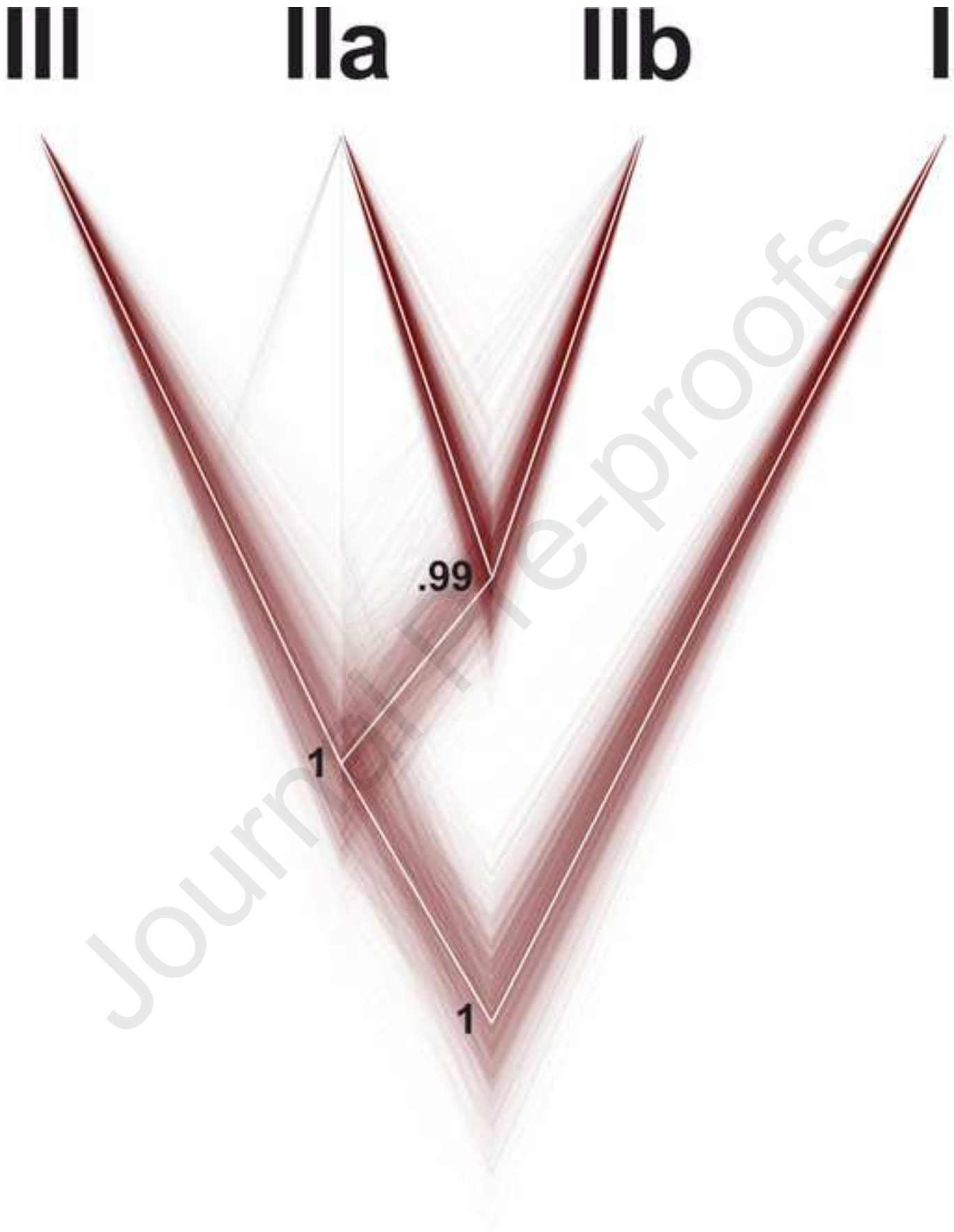

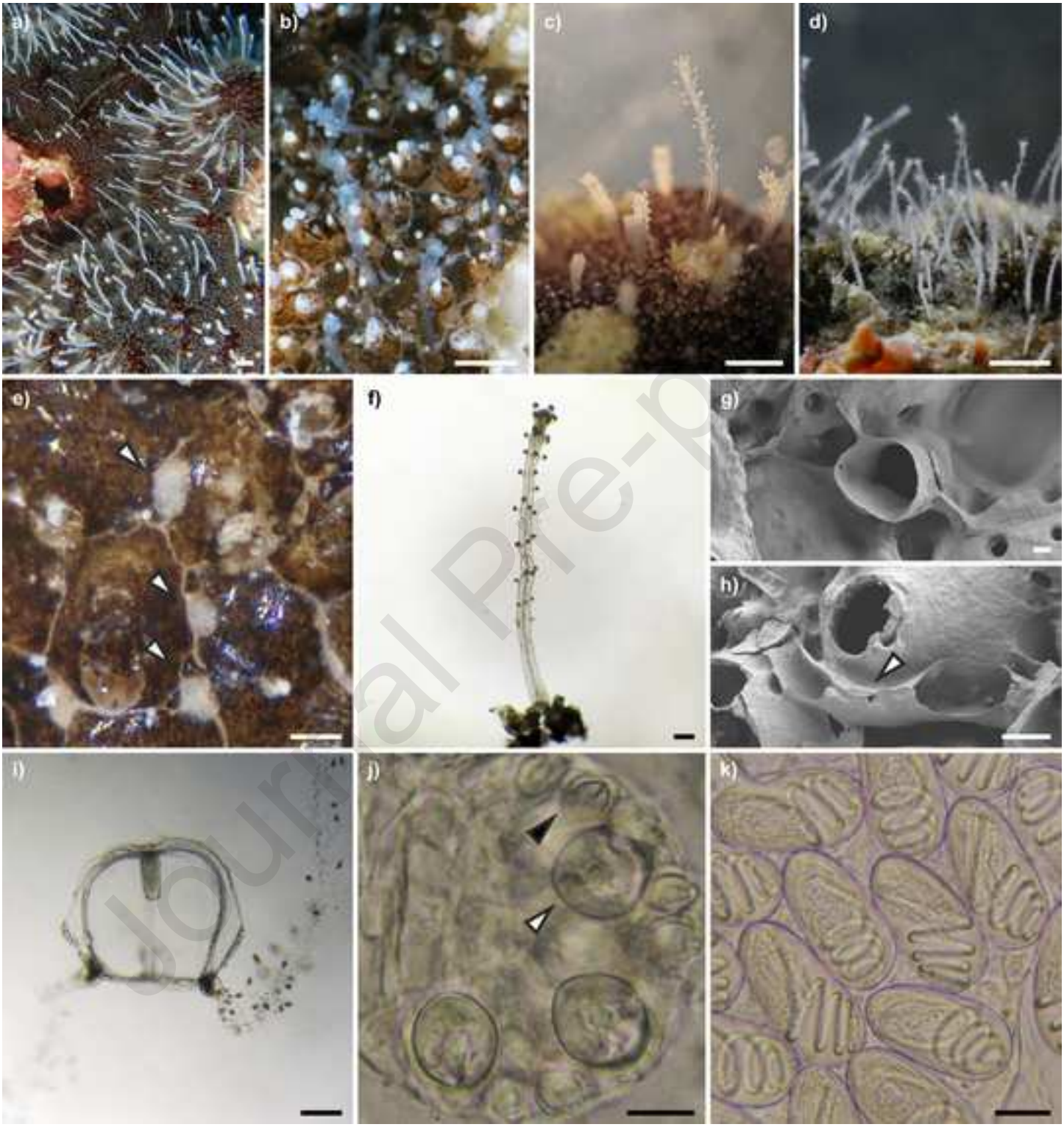

Figure 6

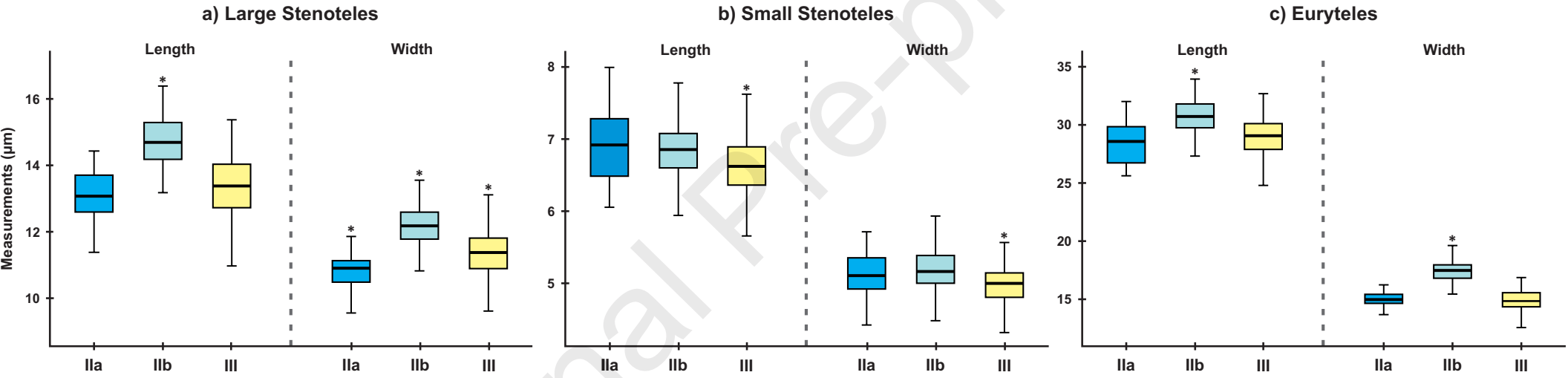

Highlights

- *Z. divergens* is a species complex associated with bryozoan genus *Celleporaria*
- General morphology is not informative
- Statistical treatment of nematocysts data revealed differences among clades
- Cryptic species show partially disjunct distribution and host specificity
- Two cryptic species have overlapping host and distribution